

Intrinsic Domain Wall Resistance in Ferromagnetic Semiconductors

Anh Kiet Nguyen, R. V. Shchelushkin, and Arne Brataas

Department of Physics, Norwegian University of Science and Technology, N-7491, Trondheim, Norway

Transport through zincblende magnetic semiconductors with magnetic domain walls is studied theoretically. We show that these magnetic domain walls have an intrinsic resistance due to the effective hole spin-orbit interaction. The intrinsic resistance is independent of the domain wall shape and width, and survives the adiabatic limit. For typical parameters, the intrinsic domain wall resistance is comparable to the Sharvin resistance and should be experimentally measurable.

Understanding magnetic topological defects is crucial in developing devices that utilize the electron spin. Domain walls are topological defects between homogeneous magnetic domains. The domain wall dynamics has traditionally been induced by external magnetic fields. There has recently been a large interest in the scientific community on current induced magnetization dynamics, where domain walls and domains change in response to applied electric currents [1]. Domain walls can also be electrically detected, by their electrical resistance. Knowledge of the domain wall's effect on the electrical resistance is important for the understanding of spin transport in condensed matter and for the electrical detection of magnetic topological defects.

Transport through domain walls have been extensively studied in metallic systems, theoretically [2] and experimentally [3]. The domain wall resistance is defined as $R_w = R - R_0$, where R and R_0 are resistances with a domain wall and with homogeneous magnetization, respectively. When the domain wall is thinner than the mean free path, in the ballistic regime, R_w is positive. In diffusive systems, when the domain wall is wider than the mean free path, the sign of the domain wall resistance is still under debate, *i.e.* the domain wall can increase or decrease the resistance of the ferromagnet. In ballistic and diffusive metal systems, R_w approaches zero with increasing domain wall width and vanishes in the adiabatic limit when the domain wall is much wider than the Fermi wavelength.

Ferromagnetic semiconductors integrate magnetization controlled spin transport with gate controlled carrier densities in semiconductors. Domain walls in these systems have been recently studied experimentally [4, 5, 6, 7]. The strong interaction between the spin of the effective holes and their orbits in dilute magnetic semiconductors changes the transport properties of magnetic domain walls qualitatively. In this Letter, we show that domain walls in zincblende magnetic semiconductors have an intrinsic resistance R_w^I which is the part of R_w that survives the adiabatic limit. R_w^I is independent of the width and detailed shape of the domain walls and is due to the effective spin-orbit interaction.

Related manifestations of the coupling between the spin-orbit interactions and the magnetizations are the anisotropic magneto resistance (AMR) [8, 9, 10, 11] and

the tunneling anisotropic magneto resistance (TAMR) [4, 13, 14]. In domain walls, some carriers are prevented by the spin-orbit interaction to adiabatically adapt to the change in the direction of the local magnetization producing a finite R_w even in the adiabatic limit. R_w^I depends mainly on three material parameters: the effective spin-orbit coupling, the exchange field and the Fermi energy. Hole transport in dilute magnetic semiconductors with strong spin-orbit interaction is usually difficult to treat analytically. Nevertheless, we find an analytical solution for the adiabatic domain wall conductance.

We model hole transport in zincblende magnetic semiconductors by the following dimensionless Hamiltonian

$$H = \alpha_1 p_i p_i - \alpha_2 (J_i J_j p_i p_j) + J_i h_i, \quad (1)$$

where the subscripts $(i, j) = x, y, z$ and the Einstein sum convention is assumed. Furthermore, $\mathbf{h}(\mathbf{r})$ is the dimensionless exchange field, describing the interaction between holes and localized magnetic moments, $|\mathbf{h}(\mathbf{r})| = h_0$. In Eq. 1, \mathbf{p} is the dimensionless momentum operator and \mathbf{J} denotes the angular momentum operator for $J = 3/2$ spins. The parameters α_1 and α_2 are controlled by the hole effective mass and the strength of the spin-orbit interaction, respectively. Their relation to the Luttinger parameters [15] γ_1 , γ_2 and γ_3 are $\alpha_1 = (\gamma_1 + 5\gamma_2/2)/(\gamma_1 - 2\gamma_2)$ and $\alpha_2 = 2\gamma_2/(\gamma_1 - 2\gamma_2)$. In our notation, energies, momentums and lengths are measured in units of the Fermi energy, Fermi momentum and Fermi wavelength of heavy holes for a given doping in the original non-magnetic host system, $h_0 = 0$. A six band version of Eq. 1 explains many features of zincblende magnetic semiconductors [16, 17, 18]. We employ the spherical approximation [19] and disregard two split-off bands. Thus, $\gamma_3 = \gamma_2$ and the Fermi energy E_F is assumed to be smaller than the split-off energy. We compute the conductance $G = 1/R$ from the Landauer-Büttiker formula $G = (e^2/h) \sum_{nm} |t_{nm}|^2$, where t_{nm} is the unit flux normalized transmission between the n and m transverse waveguide modes.

Let us first prove that holes governed by the Hamiltonian (1) exhibit an intrinsic adiabatic domain wall resistance. We separate the Hamiltonian into an intrinsic contribution \tilde{H}_I and a collision contribution \tilde{H}_C by transforming H into a local basis where the quantization axis

for \mathbf{J} is parallel to $\mathbf{h}(\mathbf{r})$, $\tilde{H} = U H U^{-1} = \tilde{H}_I + \tilde{H}_C$:

$$\begin{aligned}\tilde{H}_I &= \alpha_1 p_i p_i - \alpha_2 (\tilde{J}_i \tilde{J}_j p_i p_j) + J_z h_0, \\ \tilde{H}_C &= (\alpha_1 \delta_{ij} - \alpha_2 \tilde{J}_i \tilde{J}_j) [\kappa_i \kappa_j + \Lambda_{ij} + 2\kappa_i p_j],\end{aligned}\quad (2)$$

where $U(\mathbf{r})$ is a 4×4 unitary operator defined such that $U[\mathbf{h}(\mathbf{r}) \cdot \mathbf{J}]U^{-1} = J_z h_0$. Furthermore, $\tilde{J}_i = U J_i U^{-1}$, $\kappa_i = U p_i U^{-1}$ and $\Lambda_{ij} = p_i U p_j U^{-1}$ are 4×4 matrices that do not operate on the spatial coordinate \mathbf{r} .

Consider the adiabatic limit when the width of the domain wall λ_w is much larger than the Fermi wavelength λ_F . Hence, $\kappa_i \sim 1/\lambda_w \rightarrow 0$, $\Lambda_{ij} \sim 1/\lambda_w^2 \rightarrow 0$ and thus $\tilde{H}_C \rightarrow 0$. Without the effective spin-orbit coupling, $\alpha_2 = 0$, \tilde{H}_I is independent of directional variations in the exchange field and the domain wall resistance vanishes, $R_w = 0$. In contrast, with finite effective spin-orbit coupling, $\alpha_2 \neq 0$, \tilde{H}_I varies for systems with or without variations in the exchange field, since \tilde{J}_i differs from J_i . In other words, the spin polarization of the transport channels is anisotropic, giving rise to a finite intrinsic domain wall resistance.

In order to quantify our findings, we consider the linear response of a rectangular conductor with a cross section $A = L_x L_z$ and periodic boundary condition (PBC) along the x and z directions. Transport is along the y -axis. We consider three types of domain walls: Bloch ZX-wall, Neel ZY wall and Neel YZ-wall described by $\mathbf{h}(y) = [f_2(\tilde{y}), 0, f_1(\tilde{y})]$, $\mathbf{h}(y) = [0, f_2(\tilde{y}), f_1(\tilde{y})]$ and $\mathbf{h}(y) = [0, f_1(\tilde{y}), f_2(\tilde{y})]$, respectively. Here, $f_1(\tilde{y}) = h_0 \tanh(y/\lambda_w)$ and $f_2(\tilde{y}) = h_0 / \cosh(y/\lambda_w)$.

Translation invariance conserves the transverse momenta k_x and k_z that label the transport channels. Additionally, each (k_x, k_z) channel contains four internal spin channels originating from the four spin-orbit coupled bands. The distribution of the transport channels at position y , $T_y(k_x, k_z)$, may be found by solving the eigenvalue problem $H(k_x, y, k_z)\psi_y = E_F \psi_y$. The Fermi energy, E_F , is position independent. Due to the interplay of the spin-orbit interaction and the magnetization, the number of open channels is anisotropic in the momentum k_x - k_z space, unlike systems where the effective spin-orbit interaction vanishes. In the adiabatic limit, a conducting channel must exist throughout the system in order to contribute to the conductance. Mathematically this can be expressed as $G = (e^2/h) \sum_{k_x, k_z} T(k_x, k_y)$, where $T(k_x, k_y) = \cap_{y=-\infty}^{\infty} T_y(k_x, k_z)$ is the intersection of all distributions of transport channels as one traverses the domain wall, see Fig.1. In the case of a homogeneous ferromagnet, the conductance is $G_0 = 1/R_0 = (e^2/h) \sum_{k_x, k_z} T_{y=-\infty}(k_x, k_z)$. If and only if $T_{y=-\infty}$ is identical to or is a subset of T_y for all y then $R_w^I = 0$. This occurs only when the effective spin-orbit interaction or h_0 vanishes.

For Bloch walls, $T_y(k_x, k_z)$ is conformal under translation and simply rotates in the same direction as the exchange field, see Fig.1. Traversing from $y = -\infty$ to

∞ corresponds to a π -rotation of $T_{y=-\infty}(k_x, k_z)$ forcing $T(k_x, k_y)$ to be circular symmetric, see Fig.1. An analytical expression for the ballistic conductance through an adiabatic Bloch wall can be written as

$$G_B = \frac{e^2 A}{2\hbar} \{ \Re(k_1)^2 + \Re(k_2)^2 + \Re(k_3)^2 + \Re(k_4)^2 \} \quad (3)$$

where \Re denotes the real part and

$$\begin{aligned}k_1 &= \sqrt{(2\gamma_1 E_F + D)B}, \quad k_4 = \sqrt{(2\gamma_1 E_F - D)B} \\ k_2 &= \Xi(X_1) \sqrt{E_F - 3h_0/2} \\ &\quad + \Xi(-X_1) \sqrt{(\gamma_1 - 2\gamma_2)(2E_F + h_0)B} \\ k_3 &= \Xi(X_1) \sqrt{(\gamma_1 - 2\gamma_2)(2E_F + h_0)B} \\ &\quad + \Xi(-X_1) \Xi(X_2) \sqrt{E_F - 3h_0/2} \\ &\quad + \Xi(-X_2) \sqrt{(\gamma_1 - 2\gamma_2)(2E_F - h_0)B}\end{aligned}$$

where $\Xi(X)$ is the Heaviside step function with $\Xi(0) = 0.5$, $X_1 = (2\gamma_2 E_F)/(\gamma_1 + \gamma_2) - h_0$ and $X_2 = (4\gamma_2 E_F)/(\gamma_1 + 4\gamma_2) - h_0$. Furthermore, $B = 1/(2\gamma_1 + 4\gamma_2)$ and

$$\begin{aligned}D &= h_0(\gamma_1 - 2\gamma_2) + \\ &\quad 2\sqrt{h_0^2(\gamma_1^2 - \gamma_1\gamma_2 - 2\gamma_2^2) - 2h_0\gamma_2 E_F(\gamma_1 - \gamma_2) + 4\gamma_2^2 E_F^2}.\end{aligned}$$

For Neel walls, $T_y(k_x, k_z)$ is not conformal under translation and Eq. 3 does not apply.

Beyond the adiabatic approximation, we use a stable transfer matrix method [20] to find the conductance numerically. The system is discretized into $N_x \times N_y \times N_z$ lattice points with lattice constants a_x , a_y and a_z . We use $L_z = L_x = N_x a_x = 5$, $a_x = a_z = 0.05$, $L_y = 150$, $a_y = 0.08$ and $\gamma_1 = 6.8$. Varying γ_2 or h_0 changes the reservoir properties. We have chosen to vary the Fermi energy, $E_F(\gamma_2, h_0)$, keeping the *hole carrier density constant*, to mimic experimental conditions. $E_F(\gamma_2, h_0)$ is calculated numerically. We fixed the volume density of holes such that $E_F(\gamma_2 = 2.1, h_0 = 0) = 1$. Experimentally [17, 21], $E_F(h_0)/h_0 \sim 1$ which corresponds to $h_0 \sim 1.5$. The convergence of the numerical scheme is verified by checking the unitarity of the scattering matrix. We present our results in terms of relative domain wall resistance, $\mathcal{R}_w = (R - R_0)/R_0$.

For increasing λ_w , the direct collision between holes and the domain wall gradient decreases and $\mathcal{R}_w(\lambda_w)$ drops rapidly to its intrinsic value, Fig.1. Note that $\mathcal{R}_w(\lambda_w)$ is very close to its intrinsic value already when $\lambda_w \sim 1$ for ZX and ZY walls, and $\lambda_w \sim 0.5$ for a YZ wall *e.g.* when the domain wall width is equal or smaller than the Fermi wavelength of heavy holes.

The relative intrinsic domain wall resistance as a function of the exchange field is shown in Fig.2. Generally, $\mathcal{R}_w^I(h_0)$ increases for increasing h_0 , due to an increase in the anisotropy in $T_y(k_x, k_z)$. For the YZ wall, however, the Sharvin resistance R_0 increases even faster than R leading to a weak reduction in \mathcal{R}_w^I at large h_0 . We also

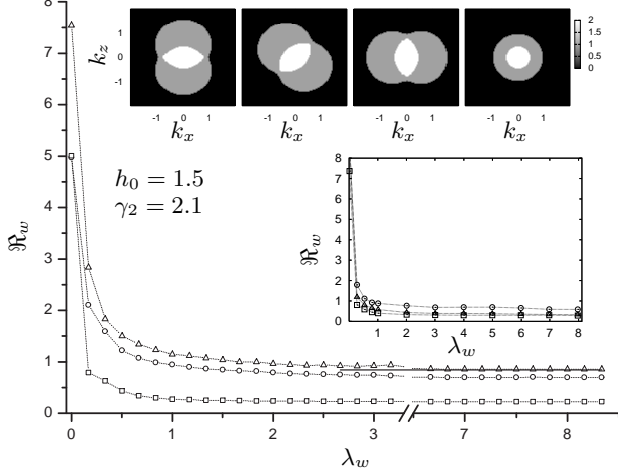


FIG. 1: Relative domain wall resistance versus wall width for ZX wall (triangle), ZY wall (circle), and YZ-wall (square). The solid line displays the intrinsic resistance derived from Eq. 3. Bottom right inset: \mathcal{R}_w for a film shaped system with Dirichlet boundary conditions. Top left to right insets: Distribution of conducting channels $T_y(k_x, k_z)$ for $y = -\infty$, $y = -0.88\lambda_w$, $y = 0$, and the intersection $T(k_x, k_z)$, for a ZX wall.

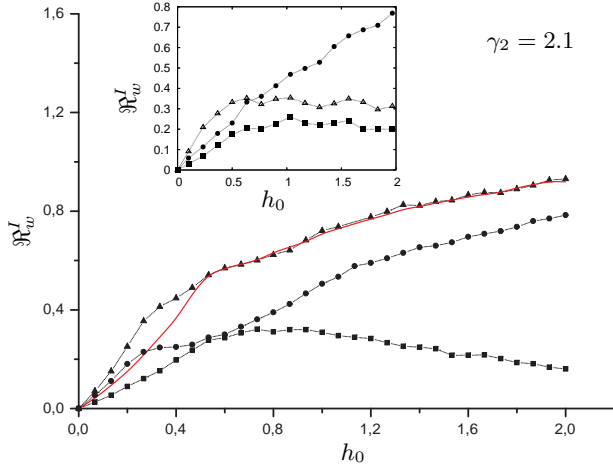


FIG. 2: Intrinsic relative domain wall resistance versus exchange field for ZX-wall (triangle), ZY-wall (circle), and YZ-wall (square). The solid line displays the analytical result for a ZX-wall, Eq. (3). Inset: $\mathcal{R}_w^I(h_0)$ for a film shaped system with Dirichlet boundary conditions.

see in Fig.2 that the numerical result for the Bloch wall is, within 2%, identical to the analytical result derived from Eq. 3 for $h_0 > 0.5$. There are small deviations at small $h_0 < 0.5$. Here, the adiabatic limit requires very large λ_w and system sizes larger than one we used, $L_y = 150$, for convergence.

The relative intrinsic domain wall resistance as a func-

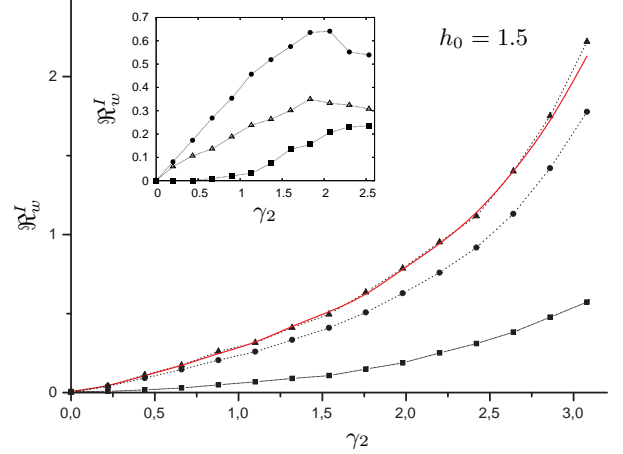


FIG. 3: Intrinsic relative domain-wall resistance as functions of hole spin-orbit coupling parameter, $\mathcal{R}_w^I(\gamma_2)$: ZX-wall (triangle), ZY-wall (circle) and YZ-wall (square). Solid line shows the analytical result for a ZX-wall. Inset: $\mathcal{R}_w^I(\gamma_2)$ for a film shaped system with Dirichlet boundary conditions.

tion of the effective spin-orbit coupling is shown in Fig. 3. $\mathcal{R}_w^I(\gamma_2)$ increases monotonically with increasing γ_2 for all walls. This is due to an increase in the anisotropy in $T_y(k_x, k_z)$. We also see that the numerical result for the Bloch wall is identical to the analytical result derived from Eq. 3 for $\gamma_2 < 2.7$. The small deviation at large $\gamma_2 > 2.7$ is caused by the same effect as previously discussed for $\mathcal{R}_w^I(h_0 < 0.5)$. Here, increasing γ_2 reduces the effective amplitude of the exchange field along certain directions.

For reasonable parameters $\gamma_2 \sim 2.1$ and $h_0 \sim 1.5$, $\mathcal{R}_w^I \sim 0.9$ and 0.7 for the ZX and ZY walls, respectively. In other words, a domain wall removes nearly half of the Sharvin conducting channels in ballistic adiabatic transport, an effect that should be clearly measurable. An interesting question is how much of the intrinsic resistance still remains in the diffusive transport regime. We know that the anisotropy in the distribution of conducting channels with respect to the direction of the exchange field do survive in the diffusive limit leading to the AMR effect [8, 9, 10, 11]. We therefore expect that at least part of the intrinsic resistance will also survive the diffusive limit. Furthermore, the intrinsic domain wall resistance is reached already for domain wall widths comparable to the Fermi wavelength. Consequently, we expect that the ballistic intrinsic domain wall resistance will be important even in rather dirty state-of-the art dilute ferromagnetic semiconductors where the mean free paths are not very much smaller than the Fermi wavelengths.

Let us explain the rigidity of the intrinsic domain wall resistance against variations in the domain wall's width and shape using topological arguments. Consider a Bloch

ZX wall. First, define the order parameter space as a two dimensional space in which two dimensional vectors map to points [22], *e.g.* the real space vector $(h_x\hat{x}+h_z\hat{z})$ maps into the point $(M_x, M_z) = (h_x, h_z)$ in the order parameter space. Second, note that the distribution of conducting channels, $T_y(k_x, k_z)$, depends on the average exchange field within a wave packet $\mathbf{h}(y) \rightarrow \bar{\mathbf{h}}(y)$. Thus, the conductance $G \sim \cap_{y=-\infty}^{\infty} T_y(k_x, k_z)$ depends on $\bar{\mathbf{h}}(y)$ or, more precisely, its mapping in the order parameter space. For $\lambda_w \ll \lambda_F$, $\bar{\mathbf{h}}(y)$ maps, approximately, into a half ellipse, $M_x^2\lambda_F^2/9\lambda_w^2 + M_z^2 = h_0^2$ where $M_x > 0$. The mapped curve becomes more circular for increasing λ_w . For $\lambda_w > \lambda_F$, $\bar{\mathbf{h}}(y)$ maps to a half circle, $M_x^2 + M_z^2 = h_0^2$ where $M_x > 0$. In this smooth (adiabatic) limit, ZX domain walls of all widths and shapes map into the same half circle, and thus have the same conductance.

So far, we have assumed periodic boundary condition in the transverse directions. Spin and orbital motion are coupled at the boundaries due to the spin-orbit interaction, which could change the results. In order to address this question, we have also numerically computed the conductance using Eq. 1 with Dirichlet boundary condition, $\psi(0, y, z) = \psi(L_x + a_x, y, z) = \psi(x, y, 0) = \psi(x, y, L_z + a_z) = 0$. To mimic experimental available 3D film shaped conductors, we use $L_x = 6$, $a_x = 1/3$, $L_z = 3$, $a_z = 3/10$ and $L_y = 100$, $a_y = 1/4\pi$. It turns out that the Dirichlet boundary condition together with small L_z prevent the development of extreme anisotropies in the distribution of conducting channels, expected at large h_0 and γ_2 . This leads to a reduction of \mathfrak{R}_w^I by a factor of 2 for the ZX wall. \mathfrak{R}_w^I for the ZY and YZ walls are less affected since the distribution of conducting channels for $\mathbf{h} \parallel \hat{y}$ is isotropic. The relative domain wall resistance as a function of λ_w is shown in the inset of Fig. 1. Similar to the PBC case, $\mathfrak{R}_w(\lambda)$ drops to its intrinsic value at $\lambda_w \sim 1$ for ZX and ZY walls, and $\lambda_w \sim 0.5$ for YZ wall. $\mathfrak{R}_w^I(h_0)$ is shown in the inset of Fig. 2. Here, \mathfrak{R}_w^I for the ZX-wall forms a plateau for $h_0 > 0.5$ above which the anisotropy in the conducting channels is prevented to develop further. We see in the inset of Fig. 3 that $\mathfrak{R}_w^I(\gamma_2)$ for the ZY and ZX walls develop a peak/plateau around $\gamma_2 \sim 2$ where the anisotropy in the conducting channels is prevented to develop further. In any case, the intrinsic resistance remains well defined and finite in a 3D film shaped conductor with Dirichlet boundary condition.

In conclusion, we have shown that dilute magnetic semiconductors exhibits an intrinsic domain wall resistance. The intrinsic domain wall resistance depends only on the map of the domain wall in the magnetic order parameter space and not on their real space width and shape. An analytical expression for the adiabatic conductance for Bloch walls is given. For typical parameters, the intrinsic domain wall resistance is comparable to the Sharvin resistance, and should therefore be experimentally measurable. The domain wall resistance drops

to its intrinsic value when λ_w approaches half the Fermi wavelength for heavy holes or a quarter of λ_F for light holes. These values are not too far from mean free path accessible presently accessible, *e.g.* in Ref. [4]. From general topological arguments, we show that topological magnetic defects have an intrinsic resistance against transport of carriers with strong spin-orbit coupling that survive the adiabatic limit.

We thank J. Schliemann, Y. Galperin, A. Sudbø, J. Hove, D. Huertas-Hernando and G. E. W. Bauer for stimulating discussions. This work has been supported in part by the Research Council of Norway through grants no. 162742/V00, 1534581/432, 1585181/143, and 1585471/431.

-
- [1] L. Berger, Phys. Rev. B **54**, 9353 (1996); J. Slonczewski, J. Magn. Magn. Mater. **159** (1996); Y. Tserkovnyak *et al.*, Rev. Mod. Phys. **77**, 1375 (2005); I. N. Krivorotov *et al.*, Science **307**, 228 (2005) and references therein.
 - [2] L. Berger, J. Appl. Phys. **55**, 1954 (1984); G. Tatara and H. Fukuyama, Phys. Rev. Lett. **78**, 3773 (1997); P. M. Levy and S. Zhang, Phys. Rev. Lett. **79**, 5110 (1997); R. P. van Gorkom, A. Brataas, and G. E. W. Bauer, Phys. Rev. Lett. **83**, 4401 (1999); G. Tatara and H. Kohno, Phys. Rev. Lett. **92**, 086601 (2004); Z. Li and S. Zhang, Phys. Rev. B **70**, 024417 (2004).
 - [3] J. F. Gregg *et al.*, Phys. Rev. Lett. **77**, 1580 (1996); N. Garcia, M. Munoz, and Y.-W. Zhao, Phys. Rev. Lett. **82**, 2923 (1999); A. Kent *et al.*, J. Phys. Cond. Mat. **13**, R461 (2001); D. Buntinx *et al.*, Phys. Rev. Lett. **94**, 017204 (2005);
 - [4] C. Rüster *et al.*, Phys. Rev. Lett. **91**, 216602 (2003).
 - [5] M. Yamanouchi *et al.*, Nature **428**, 539 (2004).
 - [6] D. Chiba *et al.*, Phys. Rev. Lett., **96**, 096602 (2006).
 - [7] H. X. Tang *et al.*, Nature **431**, 52 (2004).
 - [8] T. Hayashi *et al.*, Physica B **284**, 1175 (2000).
 - [9] D. Baxter *et al.*, Phys. Rev. B **65**, 212407 (2003).
 - [10] T. Jungwirth *et al.*, Appl. Phys. Lett. **83**, 320 (2003).
 - [11] K. Y. Wang *et al.*, Phys. Rev. B **72**, 085201 (2005).
 - [12] C. Rüster *et al.*, Phys. Rev. Lett. **94**, 027203 (2005).
 - [13] C. Gould *et al.*, Phys. Rev. Lett. **93**, 117203 (2004).
 - [14] L. Brey, C. Tejedor, and J. Fernández-Rossier, Appl. Phys. Lett. **85**, 1996 (2004).
 - [15] J. M. Luttinger, Phys. Rev. **102**, 1030 (1956).
 - [16] T. Dietl *et al.*, Science **287**, 1019 (2000).
 - [17] M. Abolfath *et al.*, Phys. Rev. B **63**, 054418 (2001).
 - [18] J. König *et al.*, in *Electronic Structure and Magnetism of Complex Materials*, edited by D. J. Singh and D. A. Papaconstantopoulos (Springer Verlag, 2002).
 - [19] A. Baldereschi and N. O. Lipari, Phys. Rev. B **8**, 2697 (1973).
 - [20] T. Usuki *et al.*, Phys. Rev. B **52**, 8244 (1995).
 - [21] F. Matsukura *et al.*, Phys. Rev. B **57**, R2037 (1998).
 - [22] P. M. Chaikin and T. C. Lubensky, *Principles of condensed matter physics* (Cambridge University Press, Cambridge UK, 1995).